Bio-Mimicry: Tree Rings and Three-Dimensional Printing – Preliminary Biomimetic Experiments with Fused Deposition Modeling Using Acrylonitrile Butadiene Styrene Filament

Murat Aydin,[a,*] and Tuğba Yilmaz Aydin [b]

Wood is a complex, natural structure and an essential source of nutrition, construction and building materials, energy, *etc.* Because of its microscopic structure, it is difficult to model its composition. In this study, the bio-mimicry of annual rings of the wood was evaluated by modeling and printing four different models with different ring diameters. The CATIA v5 software was used for 3D modeling. The designed models were additively manufactured using a 3D printer *via* the fused deposition of the acrylonitrile butadiene styrene (ABS) filament. The infill density and type, shell, layer height, and printing speed were evaluated for their influence on the structure of the ring. According to the results of preliminary biomimetic experimental, none of the models were exactly printed using the FDM method and ABS filament. Furthermore, the printing parameters did not significantly improve ring structure formation. Only the earlywood section of Model 4 could be moderately printed. Therefore, using these tools with printing parameters and materials was not found to be suitable for bio-mimicry of tree rings even if the size of the rings was multiplied by ten. In future work, the same models will be printed using different methods and tools to evaluate the printing ability or differences.

INTRODUCTION

Wood is a natural and biodegradable composite that has a complex structure formed along axes by biological elements. In the center of the structure, there is pith surrounded by circular-like annual growth rings that form the polar orthotropic nature of wood. Sequentially repeated annual rings serve as a "database" for trees; because each year is different, year-by-year growth patterns are stored in the rings. These rings are formed in response to seasonal changes (Cerda *et al.* 2007).

Environmental friendliness, cost-efficiency, and abundance are some of the outstanding features of wood and cellulose-based materials that are spotlighted for utilization in three-dimensional (3D) printing applications (Sharma *et al.* 2021). Additive manufacturing (AM) is an emerging way for printing biomimetic structures. There have been many studies focused on bio-mimicry of wood or wood-related issues, including biomimetics of living wood using AM (Thibaut 2019); wood tissue printing (Markstedt *et*

al. 2019); powder-based 3D-printing by binder jetting (BJ) of dry-wood termite frass to bio-mimic the biodegraded wood (Plarre *et al.* 2021); 3D-printed wood warped seedpod by wooden ink with polydisperse wood powder (Kam *et al.* 2022); mechanical properties of printed (stereolithography) composite composed of poplar wood flour modified with methacrylate-based resin (Zhang *et al*. 2021); review data for polylactic acid (PLA) filament modified with plant-sourced materials (Bhagia *et al.* 2021); plant-derived materials used in 3D printing (Sharma *et al.* 2021); biomass-derived 3D printing materials (Ji *et al.* 2020); robotic arms for cellulose-based filament deposition (Iyer and Hasenson 2019); and lignin types and manners of printing of lignin using AM (Ebers *et al.* 2021).

The physical and mechanical properties of wood are correlated strictly to annual rings. These features also vary within growth rings because of the differences in cell structure, and generally latewood (LW) presents higher properties (mechanical, density, and shrinkage) and darker color than the earlywood (EW) sections (Zink-Sharp 2004). The EW and LW mechanical properties (Krauss *et al.* 2011; Büyüksari *et al.* 2017), the influence of annual rings on ultrasonic wave propagation (Aydın 2022), the influence of annual ring orientation on bending strength (Rede *et al.* 2017), the influences of ring width and fiber dimension on compressive strength (Ajuziogu *et al.* 2019), and age and growth rate (Briand *et al.* 1993) are some factors that affect tree ring properties.

The complex formation and small size of the elements that form the wood structure are obstacles that make biomimetics of the annual ring difficult. Furthermore, there are limited studies focused on the AM of wooden tissue or cellular structures; Markstedt *et al.* (2019) and Malek *et al.* (2017) are two of them that used ink-based methods for cell printing. However, sequential formation of the EW and LW is an important characteristic of an annual ring, and it has not been considered in published studies. Furthermore, variation between EW and LW is one of the crucial points for physical and mechanical properties. Therefore, this study created models with different ring diameters to mimic the annual ring formation and evaluate their printability in preliminary experiments using the fused deposition modeling (FDM) method. These models do not reflect the complex polar orthotropic nature of wood. Indeed, they involve certain dimensions of cell walls and lumens with cylindrical or square shapes. Therefore, molecular level of the wood structure was not considered.

EXPERIMENTAL

Three-dimensional models of the ring structure were prepared using CATIA v5 software (Dassault Systemes SE, Velizy-Villacoublay, France). As shown in Fig. 1, four different models with different ring diameters were created. Model 1, 2, and 3 were 10 x 10 x 10 mm cubic samples with one constant (1 mm) and three different (0.4, 0.6, and 0.8 mm) ring diameters. Model 4 was sized as 5 x 20 x 10 mm through L, R, and T directions, respectively. The size through the L direction was ½ reduced to decrease unnecessary layer accumulation, and printing time was shortened.

Annual ring widths (ARW) considerable vary according to species, ranging from 1.26 to 1.37 mm (Aydın 2022), 1.34 mm (Büyüksari *et al.* 2017), 0.79 to 2.6 mm (Dündar 2005), and 0.37 to 3.91 (Sensuła *et al.* 2017) for Scots pine, 0.11 to 4.82 mm (from 1744 to 2011 - Hodul Mountain) for Black pine (Kantarci *et al.* 2013), and 2.45 to 4.11 mm for cedar (Akkemik 2003). Furthermore, cell wall thickness and lumen diameter greatly vary according to species, growing conditions, *etc*., and poplar has larger ring widths. Modeling

such a small structure using software is not easy and realizing such complex models by FDM is doubtful. Therefore, choosing a species that has larger ARWs (cell wall thickness and lumen diameter) and multiplying the values may be a possible solution for modeling. From this point of view, *Salix psammophila* has a 7.37 µm cell lumen diameter and 2.29 µm cell wall thickness (Zhou *et al.* 2017), and it was referenced for creating Model 4 using adapted cell wall thickness and lumen diameter values multiplied by ten. As shown in Fig. 1, the cell wall thickness and lumen diameter of EW section of Model 4 were 0.2 and 0.7 mm, respectively. For latewood, these values were 0.55 and 0.3 mm. The percentage of LW was set to approximately 1/3 of ARW in accordance with the reported 31.2/100 ratio for yellow poplar (Uzcategui *et al.* 2020). Transition changes in EW and LW were not taken into consideration, and exact same repetitions were used to provide a homogeneous structure. Other anatomical elements were overlooked in the modeling.
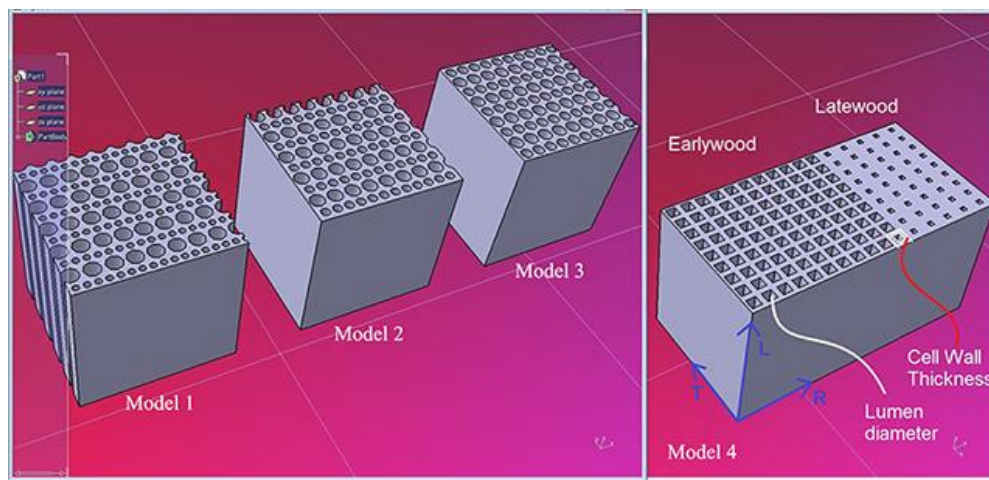

Fig. 1. 3D models with different size, shape, and sequence

A Da Vinci 1.0 AIO 3D printer (0.4 mm nozzle diameter, XYZ Printing, New Kinpo Group, Taiwan) and acrylonitrile butadiene styrene (ABS) filament (1.75 mm diameter) were used for AM by the FDM method. The characteristics of the ABS filament are presented in Table 1.

Table 1. Properties of ABS Filament

Density (g/cm³)	Diameter (mm)	Color	Thermal Properties - Temperature (°C)					
			Glass	Nozzle	Printing	Printing Bed	Softening	Melting
1.03	1.75±0.05	White	70-90	210	220-240	90-120	105	200

The resolution was set to 100 µm. Actual extruder and platform (bed) temperatures in printing were around 214 °C and 90 °C, respectively. The three of six 10 mm cubic samples were printed using default excellent printing quality parameters (30% infill density, rectilinear infill type, normal shell, 0.2 mm layer height, and slow speed). The remaining cubic samples were printed using 0.1 mm layer height to evaluate the influence of layer thicknesses on the models' structures.

Due to 21% and 25% higher tensile and flexural strength and 18% and 20% higher tensile and flexural stiffness values (XYZ Printing 2019), cellular infill form should be

chosen but due to limitations, rectilinear and honeycomb infill types were used (Fig. 2). Increasing the infill percentage strengthens the model for structural uses instead of printing non-functional parts. To evaluate the influence of infill density on ring forming, three different infill densities were used, as shown in Table 2.
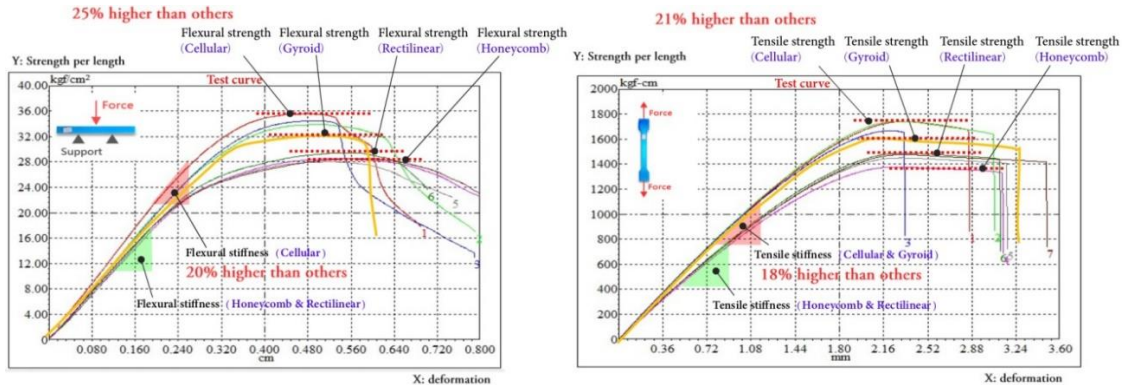

Fig 2. Strength and stiffness comparison of the infill types

Table 2. Printing Parameters for Biomimetic of Model 4

Printing Parameter	Sample A	Sample B	Sample C	Sample D	Sample E	Sample F
Infill density (%)	0	25	50	0	25	50
Infill type	Rectilinear	Rectilinear	Rectilinear	Honeycomb	Honeycomb	Honeycomb
Shell	Thin	Thin	Thin	Thin	Thin	Thin
Layer height (mm)	0.1	0.1	0.1	0.1	0.1	0.1
Speed	Slow and Fast	Slow	Slow	Slow	Slow	Slow

The shell is the outer walls of the printed part, and the strength of the printed part can be improved by increasing the shell thickness. Evaluating the mechanical properties of the models was not one of the motivations of this study. As shown in the 3D designs, the lumen diameters were too small, and selecting as thin as possible shell thickness may provide better printing of hollow shapes. The layer thickness was 0.1 mm, and printing was performed at slow speed. However, Sample A was also printed using the same parameters but with fast printing speed to compare formation.

RESULTS AND DISCUSSION

The model, print preview, and printed samples of Models 1, 2, and 3 are presented in Fig. 3. Neither previews nor printed samples reflected the model structures. The 0.4 mm rings of the Model 1 were filled by ABS. When the diameter of the rings increased, filling percentage decreased, as in Model 2. Surprisingly, it was expected that rings could be printed more accurately when the ring diameter increased to 0.8 mm, but large holes formed by merging the 1 mm and 0.8 mm rings. Furthermore, significant improvements were not observed when the samples were printed using 0.1 mm layer thickness.
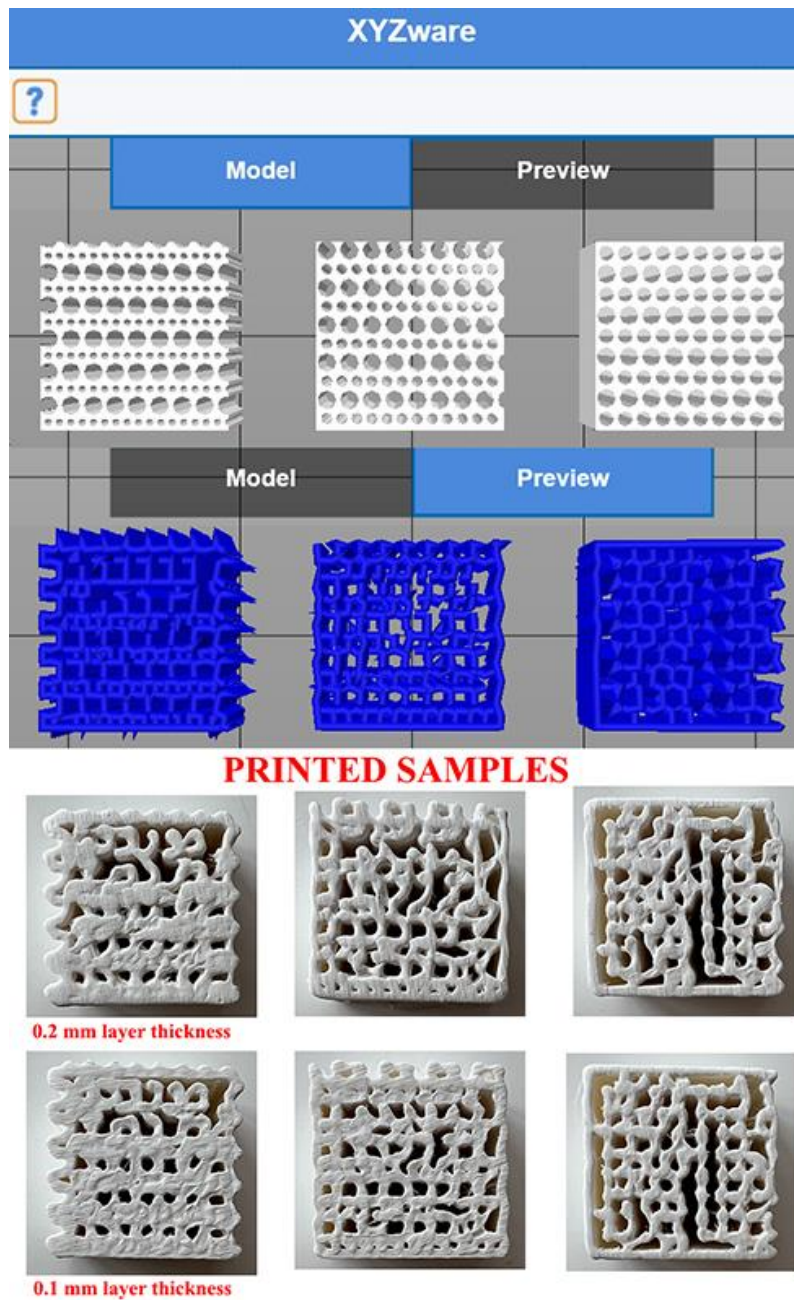
Fig. 3. Screenshots for XYZware software (models and previews) and printed samples (left to right; Model 1, 2, and 3)

Tangential-radial plane views of the printed samples (A-F) of Model 4 are presented in Fig. 4. When compared with Models 1-3, a more accurate ring structure was obtained particularly for the EW section.
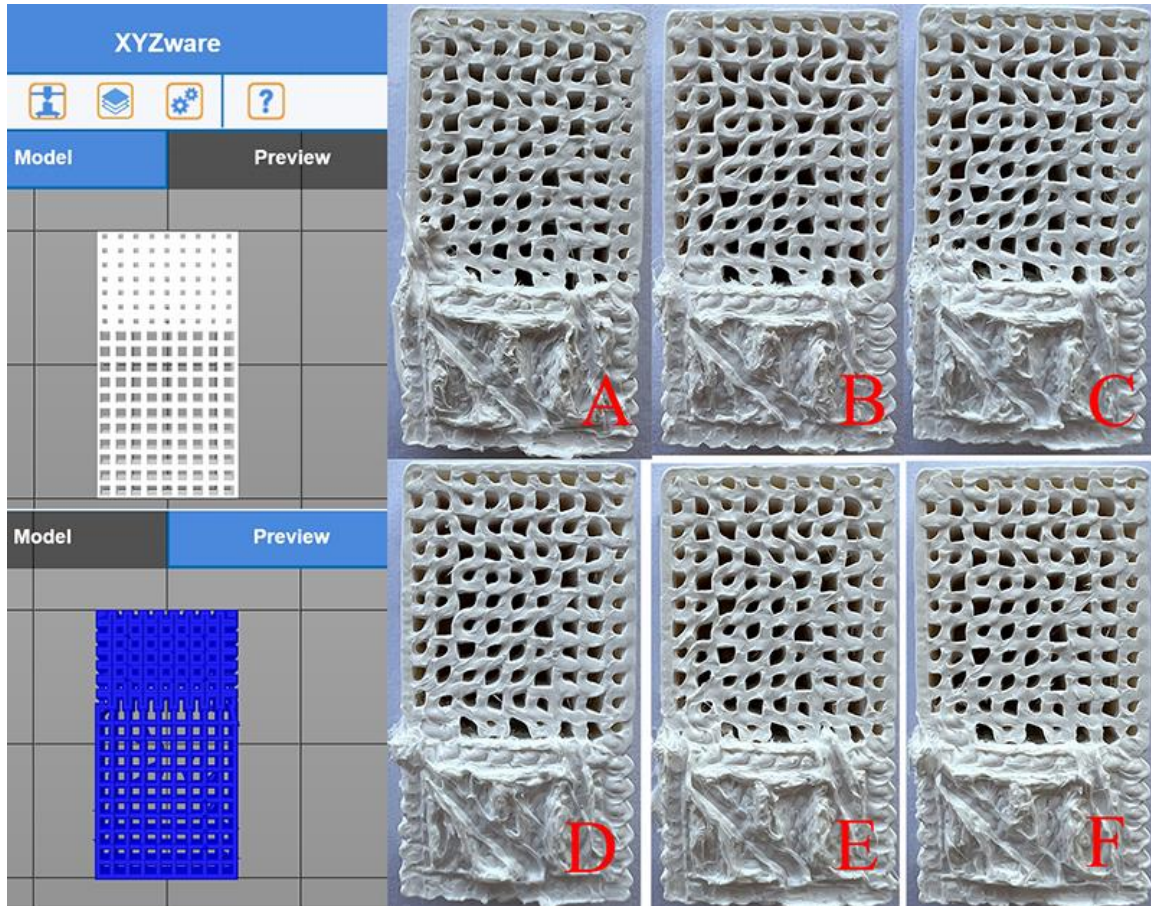
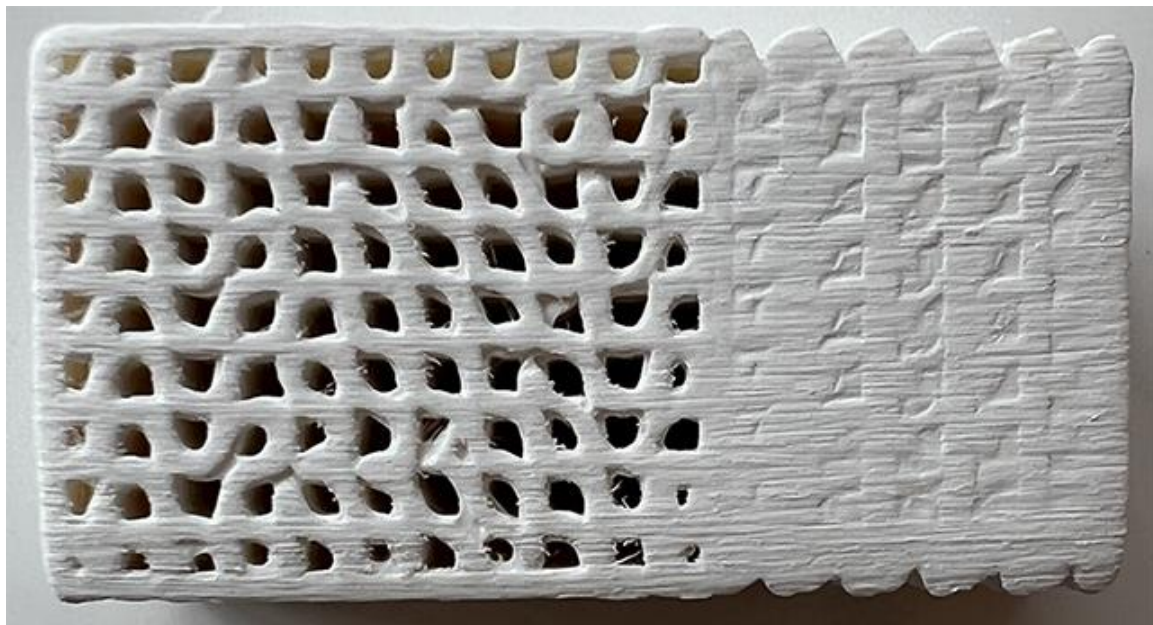**Fig. 4.** Model 4 prints with different parameters

Fig. 5. The sanded surface of a printed Model 4

However, the hollow tubes with small diameters could not be formed by the default hardware of the printer and ABS was filled in the holes. As shown in the A-F views, infill density and type did not cause significant improvements in printing processes. The surface of the model was sanded to remove overprinted material to observe the LW structure of the model (Fig. 5). As observed for Model 1, gaps with a small diameter could not be printed properly; gaps were filled by overprinted ABS.

Varied cell numbers in the layer are assumed as the reason for the annual growth ring width variation, while each cell is nearly the same size and presents almost equal mechanical features (Golovin *et al.* 2022). In additive manufacturing, surface roughness and mechanical properties of the 3D printed products are directly related to infill pattern and density. In this study, three different infill densities (0%, 25%, and 50%) were used. As shown in Fig. 4, the influence of infill on the model formation is not perceptible. In contrast, increasing infill density causes an increase in printing time.

The impact value of the cellular infill is 2102 J/m², while gyroid, honeycomb, and rectilinear infill types have 1847, 1827, and 1725J/m², respectively (XYZ Printing 2019). The cellular infill may be chosen if there is availability to provide higher impact strength. In this study, only rectilinear and honeycomb infill types were available.

Markstedt *et al.* (2019) printed a slice of wood tissue using xylan-modified cellulose nanofibril inks by extrusion-based printing with pneumatic and microvalve dispensing printer heads. The shape of the cellular structure looked as it should be, but when the size of the gaps (considerable higher than 5 mm) is taken into consideration, the diameters of the rings (particularly for Model 4) printed in this study were remarkably lower. Thus, a failure in layer formation due to relatively small ring diameters is assumed as the beginning of the improper ABS material deposition. This is one of the main reasons for unsuccessful sequential deposition in the course of bio-mimicry experiments. Maybe with the help of a relatively higher (0.4 mm) nozzle diameter, faulty sequential deposition caused irregular shape formation of the models.

Square and hexagon shaped cells with considerable higher dimensions were printed by Malek *et al.* (2017) using an ink-based method. However, cell wall thickness properties were not mentioned, while nozzle diameter was 610 µm.

More detailed models for the cellular structure of wood were designed and printed (FDM using ABS) by Ufodike *et al.* (2021) presenting the pits on the radial wall of the tracheid. The dimension of the base unit cells was around 70x65x60 mm in the Z, X, and Y directions, respectively, and the cell size was significantly higher than in this study.

Kam *et al.* (2022) concluded that structures (3D wood warped seedpod) can be successful AM by deposition of 1 mm thick layers using water-based inks in the 3D printing application. In this study, successful printing was not achieved for annual ring formation, but success can be obtained by printing models with larger ring diameters, as in previous studies. Furthermore, it is apparent that advances in this area can lead to significant improvements in the near future. Gurung (2017) stated that due to the establishment of several new businesses and competitiveness, printing quality and cost have increased and decreased, respectively. Moreover, wood or wood-based printing materials that advance the 3D printing outcomes have been effectively used in AM (Sharma *et al.* 2021), and samples manufactured in this study can be printed using such materials for a more realistic appearance.

Following this study, other AM methods such as selective laser sintering/melting and different filaments such as PLA are going to be used for printing the same models for comparison.

CONCLUSIONS

1. Specific to the used printer, materials, printing parameters, and model structures, tree rings could not be printed as they should be using fused deposition modeling (FDM). However, the earlywood (EW) section of Model 4 was moderately printed.

2. There was no significant influence of printing parameters (Table 2) on the ring formation.

3. The nozzle diameter had a great influence on the printing of the model, and the default diameter of the printer nozzle caused improper printing of rings or overprinting of the acrylonitrile butadiene styrene (ABS) filament on the latewood (LW) section.

4. This study was a preliminary biomimetic experimental of wood annual ring formation with different diameters and geometries. A comprehensive study is underway to manufacture the same models using different tools and methods of additive manufacturing for comparison.

ACKNOWLEDGMENTS

REFERENCES CITED

Ajuziogu, G. C., Onyeke, C. C., Ojua, E. O., Amujiri, A. N., and Ibeawuchi, C. C. (2019). "Effect of growth ring width and fiber dimensions on the compressive strength of some members of the Moraceae family," *Wood and Fiber Science* 51(4), 416-423. DOI: 10.22382/wfs-2019-039

Akkemik, Ü. (2003). "Tree rings of *Cedrus libani* at the northern boundary of its natural distribution," *IAWA Journal* 24(1), 63-73. DOI: 10.1163/22941932-90000321

Aydın, M. (2022). "Effects of annual ring number and width on ultrasonic waves in some softwood species," *BioResources* 17(1), 1745-1763. DOI: 10.15376/biores.17.1.1745-1763

Bhagia, S., Bornani, K., Agarwal, R., Satlewal, A., Ďurkovič, J., Lagaňa, R., Bhagia, M., Yoo, C. G., Zhao, X., Kunc, V., Pu, Y., Ozcan, S., and Ragauskas, A. J. (2021). "Critical review of FDM 3D printing of PLA biocomposites filled with biomass resources, characterization, biodegradability, upcycling and opportunities for biorefineries," *Applied Materials Today* 24. DOI: 10.1016/j.apmt.2021.101078

Briand, C. H., Posluszny, U., and Larson, D. W. (1993). "Influence of Age and growth rate on radial anatomy of annual rings of *Thuja occidentalis* L. (Eastern white cedar)," *International Journal of Plant Sciences* 154(3), 406-411. DOI: 10.1086/297122

Büyüksarı, Ü., As, N., and Dündar, T. (2017). "Mechanical properties of earlywood and latewood sections of scots pine wood," *BioResources* 12(2), 4004-4012. DOI: 10.15376/biores.12.2.4004-4012

Cerda, M., Hitschfeld-Kahler, N., and Mery, D. (2007). "Robust tree-ring detection," *Lecture Notes in Computer Science (including subseries Lecture Notes in Artificial*

Intelligence and Lecture Notes in Bioinformatics), 4872 LNCS, 575-585. DOI: 10.1007/978-3-540-77129-6_50

Dündar, T. (2005). *The Effect of Different Silvicultural Treatments on Some Technological Properties of Scotch Pine (Pinus sylvestris L.) Wood in Turkey*, Ph.D. Dissertation, İstanbul University, İstanbul, Turkey.

Ebers, L. S., Arya, A., Bowland, C. C., Glasser, W. G., Chmely, S. C., Naskar, A. K., and Laborie, M. P. (2021). "3D printing of lignin: Challenges, opportunities and roads onward," *Biopolymers* 112(6). DOI: 10.1002/bip.23431

Golovin, Y. I., Tyurin, A. I., Golovin, D. Y., Samodurov, A. A., Matveev, S. M., Yunack, M. A., Vasyukova, I. A., Zakharova, O. V., Rodaev, V. V., and Gusev, A. A. (2022). "Relationship between thermal diffusivity and mechanical properties of wood," *Materials* 15(2). DOI: 10.3390/ma15020632

Gurung, D. (2017). *Technological Comparison of 3D and 4D Printing,* Ph.D. Dissertation, Arcada University of Applied Sciences, Helsinki, Finland.

Iyer, S., and Hasenson, R. (2019). *3D Printing Using an Industrial Robotic Arm and a Cellulose Based Filament*, Master's Thesis, KTH Royal Institute of Technology, Stockholm, Sweeden.

Ji, A., Zhang, S., Bhagia, S., Yoo, C. G., and Ragauskas, A. J. (2020). "3D printing of biomass-derived composites: Application and characterization approaches," *RSC Advances* 10(37), 21698-21723. DOI: 10.1039/d0ra03620j

Kam, D., Levin, I., Kutner, Y., Lanciano, O., Sharon, E., Shoseyov, O., and Magdassi, S. (2022). "Wood warping composite by 3D printing," *Polymers* 14(4). DOI: 10.3390/polym14040733

Kantarci, M. D., Kilci, M., Akbin, G., Sayman, M., and Bircan, E. (2013). "Relationship between the annual ring widths of an old black pine (*Pinus nigra* Arnold subsp. *pallasiana*) tree and dry climate periods of Hodul Mountain forest remnants in Ürgüp/Akçaören-Turkey," in: *Proceedings of the 6th Atmospheric Science Symposium (ATMOS-2013)*, İstnabul, Turkey, pp. 15.

Krauss, A., Moliński, W., Kúdela, J., and Čunderlík, I. (2011). "Differences in the mechanical properties of earlyand latewood within individual annual rings in dominant pine tree (*Pinus sylvestris* L.)," *Wood Research* 56(1), 1-12.

Malek, S., Raney, J. R., Lewis, J. A., and Gibson, L. J. (2017). "Lightweight 3D cellular composites inspired by balsa," *Bioinspiration and Biomimetics* 12(2). DOI: 10.1088/1748-3190/aa6028

Markstedt, K., Håkansson, K., Toriz, G., and Gatenholm, P. (2019). "Materials from trees assembled by 3D printing - Wood tissue beyond nature limits," *Applied Materials Today* 15, 280-285. DOI: 10.1016/j.apmt.2019.02.005

Plarre, R., Zocca, A., Spitzer, A., Benemann, S., Gorbushina, A. A., Li, Y., Waske, A., Funk, A., Wilbig, J., and Günster, J. (2021). "Searching for biological feedstock material: 3D printing of wood particles from house borer and drywood termite frass," *PLoS ONE* 16(2 February 2021). DOI: 10.1371/journal.pone.0246511

Rede, V., Essert, S., and Kodvanj, J. (2017). "Annual ring orientation effect on bending strength of subfossil elm wood," *Journal of Wood Science* 63(1), 31-36. DOI: 10.1007/s10086-016-1596-x

Sensuła, B., Wilczyński, S., Monin, L., Allan, M., Pazdur, A., and Fagel, N. (2017). "Variations of tree ring width and chemical composition of wood of pine growing in the area nearby chemical factories," *Geochronometria* 44(1), 226-239. DOI: 10.1515/geochr-2015-0064

Sharma, V., Roozbahani, H., Alizadeh, M., and Handroos, H. (2021). "3D printing of plant-derived compounds and a proposed nozzle design for the more effective 3D FDM printing," *IEEE Access* 9, 57107-57119. DOI: 10.1109/ACCESS.2021.3071459

Thibaut, B. (2019). "Three-dimensional printing, muscles, and skeleton: Mechanical functions of living wood," *Journal of Experimental Botany* 70(14), 3453-3466. DOI: 10.1093/jxb/erz153

Ufodike, C. O., Ahmed, M. F., and Dolzyk, G. (2021). "Additively manufactured biomorphic cellular structures inspired by wood microstructure," *Journal of the Mechanical Behavior of Biomedical Materials* 123. DOI: 10.1016/j.jmbbm.2021.104729

Uzcategui, M. G. C., Seale, R. D., and França, F. J. N. (2020). "Physical and mechanical properties of hard maple (*Acer saccharum*) and yellow poplar (*Liriodendron tulipifera*)," *Forest Products Journal* 70(3), 326-334. DOI: 10.13073/FPJ-D-20-00005

XYZ Printing. (2019). "The cellular infill- our newly developed type for making stronger, high-performing FDM 3D printed parts," (https://www.xyzprinting.com/en-US/news/SWInfillTypeCellular), Accessed 11 June 2022.

Zhang, S., Bhagia, S., Li, M., Meng, X., and Ragauskas, A. J. (2021). "Wood-reinforced composites by stereolithography with the stress whitening behavior," *Materials and Design* 206. DOI: 10.1016/j.matdes.2021.109773

Zhou, X.-W., Wang, Y.-R., Wang, L., Lv, H., Zhao, R.-J., Yao, L.-H., and Chen, Z.-J. (2017). "Cell wall structure and mechanical properties of *Salix psammophila*," *Wood Research* 62(1), 1-12.

Zink-Sharp, A. (2004). "Wood formation and properties: Formation and structure of wood," in: *Encyclopedia of Forest Sciences*, J. Burley (ed.), Academic Press, Elsevier, pp. 1806-1815. DOI: 10.1016/b0-12-145160-7/00037-5